EPAPS supplementary material for "Nanophotonic control of Förster resonance energy transfer efficiency"

Christian Blum,[1] Niels Zijlstra,[1] Ad Lagendijk,[2,3] Martijn Wubs,[4]
Allard P. Mosk,[2] Vinod Subramaniam,[5] and Willem L. Vos[2]

[1]*Nanobiophysics (NBP), MESA+ Institute for Nanotechnology, University of Twente, 7500 AE Enschede, The Netherlands**
[2]*Complex Photonic Systems (COPS), MESA+ Institute for Nanotechnology, University of Twente, 7500 AE Enschede, The Netherlands*
[3]*FOM-Institute AMOLF, Science Park, 1098 XG Amsterdam, The Netherlands*
[4]*Department of Photonics Engineering, Technical University of Denmark, DK-2800 Kgs. Lyngby, Denmark*
[5]*Nanobiophysics (NBP), MIRA Institute for Biomedical Engineering and Technical Medicine and MESA+ Institute for Nanotechnology, University of Twente, 7500 AE Enschede, The Netherlands*

In this supplementary material, we describe the experimental procedures and the background theory. In the first part, we discuss the sample preparation, and we describe the molecular FRET pairs that are used. The instrumentation and the measurement procedure are explained. We discuss the characterization of the optical properties of the donor molecules. We characterize the FRET properties for the reference case (LDOS = 1), notably the Förster radius and the energy transfer efficiency. In the second part, we theoretically investigate the relation between the Förster energy transfer rate and the local density of states (LDOS) in a photonic medium. For media where material dispersion is negligible in the overlap region of the donor and acceptor spectra, we find an exact expression of the Förster transfer rate as a frequency integral over the imaginary part of the Green function. In combination with the well-known relation between the LDOS and the imaginary part of the Green function, this leads to an approximate expression of the Förster energy transfer rate in terms of a frequency integral over the LDOS. We find that Förster energy transfer rates are practically unaffected by changing the optical LDOS in a photonic medium, when keeping fixed the subwavelength local dielectric environment of the donor-acceptor pair.

PART I: EXPERIMENTAL METHODS

Sample preparation

To control the LDOS, we used planar single mirror samples. In short (for details see Ref. [2]): First, the chromium, silver, and silicon oxide layers were fabricated using multilayer e-gun deposition on a silicon wafer, carried out in a Balzers BAK 600 e-gun evaporation machine. The thickness of the SiO_2 layer was varied to control the distance between the mirror layer and the emitters. The thickness of the layers was determined using scanning electron microscopy (SEM) within an estimated error of 5%. The thickness of the layers was found to be homogeneous over the analyzed cross sections. The refractive index of SiO_2 was determined to be $n = 1.46 \pm 0.05$ by white light ellipsometry. On top of the SiO_2 spacer layer, we spincoated a thin layer of polyvinyl alcohol (PVA, $n = 1.50 \pm 0.01$). The PVA was 2% by weight dissolved in water and contained the DNA FRET pairs at low concentrations, 1 μM. The estimated distance between FRET pairs is 25 nm. We spincoated the PVA layer at 6000 rpm for 10 seconds, resulting in a homogeneous layer thickness of $17 \pm 3nm$. The thickness of the PVA layer results in a random orientation of the sampled emitters while at the same time it adds little distance uncertainty. Finally, a thick (>1 μm) layer of polymethyl methacrylate (PMMA, $n = 1.49 \pm 0.01$) was spincoated at 2800 rpm for 10 seconds on top of the PVA layer to avoid reflections from the PVA/air interface.

DNA FRET pair

We used the fluorescent dyes Atto488 and Atto565 as donor and acceptor, respectively. The dyes are coupled through a DNA strand of 15 bases: Atto488 - CGA CTC CGA GTC AGC - Atto565. The unlabeled complementary strand was used to assure the mechanical stability of the system. The HPLC and PAGE purified single-stranded DNA was obtained from IBA Biotagnology (Germany). The double-stranded DNA was formed by mixing the labeled DNA, the unlabeled complementary strand, and buffer (5 mM Tris, 100 mM NaCl). The mixture was heated to 80 °C for 10 minutes and then annealed by slowly cooling to room temperature.

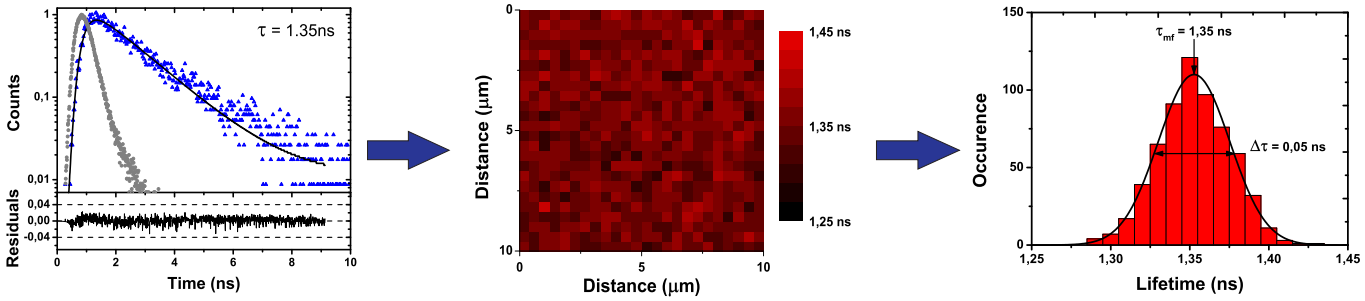

FIG. 1: **(a)** Typical decay curve measured for the FRET pair at 60 nm from a silver mirror (blue triangles), measured at $525 \pm 15nm$. The solid black line is the single-exponential fit to the data. The grey circles correspond to the instrument response function (IRF) of the system. The residuals are plotted at the bottom and show the good quality of the fit in the whole decay range. **(b)** Typical lifetime image, showing a uniform distribution of the lifetimes. Each pixel represents the lifetime extracted from a fit similar to the one shown in (a). **(c)** The lifetime histogram obtained from the lifetime image in (b). The histogram shows a narrow Gaussian distribution indicating a good sample preparation.

Instrumentation

Time-correlated single-photon counting (TCSPC) measurements were performed using a custom-built inverted confocal microscope. As excitation source, we used a pulsed diode laser operating at 485 nm at a repetition rate of 20 MHz (LDH-D-C-485, Picoquant). An epi-illumination configuration was used: the sample was illuminated and the emission was collected through the same microscope objective (LUCPlanFLN 40x, 0.6 NA , Olympus). Remaining excitation light in the detection path was blocked with a long pass filter (RazorEdge, 488 nm, Semrock) and an additional single-notch filter (Stopline, 488/14 nm, Semrock). To perform time-resolved fluorescence measurements, the emission was focused onto the active area of a single photon avalanche diode (SPCM-APQR-16, PerkinElmer), connected to the TCSPC module (PicoHarp300, Picoquant). To limit the detection wavelength to the peak of the FRET donor fluorophore, we used a band pass filter centered at 525 nm with a bandwidth of 15 nm (BrightLine, 525/15 nm, Semrock). The integration time per decay curve was chosen such that the total counts per decay curve exceeded a minimum of 20000 counts to assure accurate determination of the characteristic lifetime [1].

Measurement procedure

We scanned three areas of 50 by 50 μm and collected an average of 400 decay curves per area, see Figure 1. Each decay curve was fitted with a single-exponential decay. The quality of the fit was determined by the reduced chi-square parameter. From the determined lifetimes, we obtained one histogram per area. The distribution of lifetimes is fitted with a Gaussian distribution. A narrow distribution compared to the most frequent lifetime indicates a good sample quality. Small variations in the refractive index and in the thickness of the spacer layer will result in small deviations in the measured decay rate. If these variations are too large due to bad sample preparation, the distribution will be broad compared to the most frequent decay rate. The most frequent decay rate, *i.e.*, the peak value of the distribution, was used to calculate the decay rate, whereas the error for the decay rate was represented by the width of the distribution, typically $\Delta\tau = 0.09$ ns. From the most frequent decay rate and width of the distribution of the three areas, we determined the average decay rate and error.

CHARACTERIZATION OF THE DONOR ATTO488

For the analysis of the FRET efficiency, the quantum efficiency Q_{D} and nonradiative decay rate γ_{nr} of the donor Atto488-DNA is needed. More details about the analysis can be found in Ref. [2].

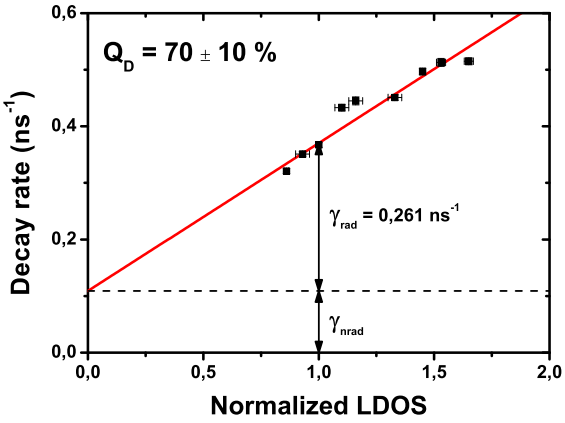

FIG. 2: Total decay rate of Atto488-DNA versus the normalized LDOS. The solid line represents a linear fit as expected from Fermi's Golden Rule. From the fit, we derived the nonradiative decay rate $\gamma_{\rm nr} = 0.109 \pm 0.029$ ns^{-1} and the radiative decay rate $\gamma_{\rm rad} = 0.261 \pm 0.025$ ns^{-1}, resulting in a quantum efficiency $Q_{\rm D} = 70 \pm 10\%$.

FÖRSTER DISTANCE AND TRANSFER EFFICIENCY OF THE ATTO488 - ATTO565 FRET PAIR

The transfer efficiency of a FRET pair can be calculated using

$$\eta_{\rm FRET} = \frac{1}{1 + \left(\frac{R}{R_0}\right)^6} \tag{1}$$

where R is the distance between donor and acceptor and R_0 is the Förster distance for the donor-acceptor pair.

The dye distributor Atto-Tec (Germany) determined the Förster distance for the Atto488-Atto565 pair as 6.3 nm. Taking into account that our samples have a higher refractive index (1.46 compared to 1.33) and the lower donor quantum efficiency as a consequence of the binding to DNA (70% compared to 80%), we calculated a Förster distance of 5.8 nm. Both donor and acceptor are attached via a 6C linker to respectively the 3' and 5' ends of the same DNA strand of a 15 base pairs long double-stranded DNA helix. Since 10 base pairs is a complete helical twist, the dyes are exactly on opposite sides of the helix. Including the length of the linkers, this results in a total distance between donor and acceptor of 6.8 nm [3] while the orientation factor κ^2 only minimally deviates from its mean value of $\kappa^2 = 2/3$ [4]. Using 5.8 nm for the Förster distance and 6.8 nm for the separation between donor and acceptor, the expected energy transfer efficiency is 28%. This value agrees well with the energy transfer efficiency of 34%, which corresponds to a Förster distance of $R_0 = 6.1$ nm for two emitters separated by 6.8 nm, determined in our experiment.

PART II: FÖRSTER TRANSFER IN TERMS OF IM[G]

The main question in this section is whether changes in the optical LDOS will affect the Förster energy transfer rate. To answer this, let us first recall how both spontaneous-emission rates and energy-transfer rates can be expressed in terms of the Green function (or more precisely Green tensor) of a nanophotonic medium.

First, the medium-dependent spontaneous-decay rate $\gamma(\mathbf{r}, \Omega)$ of an emitter at position $\mathbf{r}$ with dipole moment $\boldsymbol{\mu} = \mu\hat{\boldsymbol{\mu}}$ and transition frequency Ω can be expressed in terms of the imaginary part of the Green function $\mathbf{G}(\mathbf{r}, \mathbf{r}, \Omega)$ of the medium as

$$\gamma(\mathbf{r}, \Omega) = -\left(\frac{2\Omega^2}{\hbar\varepsilon_0 c^2}\right) \boldsymbol{\mu}^* \cdot \mathrm{Im}[\mathbf{G}(\mathbf{r}, \mathbf{r}, \Omega)] \cdot \boldsymbol{\mu} \tag{2}$$

or alternatively $\gamma(\mathbf{r}, \omega, \boldsymbol{\mu}) = (\pi\mu^2\Omega/(\hbar\varepsilon_0))N(\mathbf{r}, \omega, \hat{\mu})$ in terms of the dipole orientation dependent local optical density of states (LDOS) $N(\mathbf{r}, \omega, \hat{\boldsymbol{\mu}})$.

Second, following Dung, Knöll, and Welsch[5] the total energy transfer rate between a donor and an acceptor

molecule embedded in a frequency-dispersive and absorbing photonic medium is given by

$$W = \int \mathrm{d}\omega\, \sigma_A(\omega)\, |w(\omega)|^2\, \sigma_D(\omega), \tag{3}$$

where $\sigma_{\mathrm{D,A}}(\omega)$ are the free-space donor and acceptor spectra [5, 6]. All the effects of the photonic environment are contained in the factor $w(\omega)$ which can be expressed in terms of the Green function $\mathbf{G}(\mathbf{r}_\mathrm{A}, \mathbf{r}_\mathrm{D}, \omega)$ of the medium and the donor/acceptor dipole moments $\boldsymbol{\mu}_{\mathrm{D,A}}$ as the transfer amplitude squared

$$|w(\omega)|^2 = \left(\frac{2\pi}{\varepsilon_0}\right)\left(\frac{\omega}{\hbar c}\right)^2 \; |\boldsymbol{\mu}_\mathrm{A}^* \cdot \mathbf{G}(\mathbf{r}_\mathrm{A}, \mathbf{r}_\mathrm{D}, \omega) \cdot \boldsymbol{\mu}_\mathrm{D}|^2. \tag{4}$$

This expression sums up resonant and Förster energy transfer processes. The squared Förster transfer amplitude $|w_{\mathrm{Förster}}(\omega)|^2$ that dominates the energy transfer at subwavelength distances is given by

$$|w_{\mathrm{Förster}}(\omega)|^2 = \left(\frac{2\pi}{\varepsilon_0}\right)\left(\frac{\omega}{\hbar c}\right)^2 \; |\boldsymbol{\mu}_\mathrm{A}^* \cdot \mathbf{G}_\mathrm{S}(\mathbf{r}_\mathrm{A}, \mathbf{r}_\mathrm{D}, \omega) \cdot \boldsymbol{\mu}_\mathrm{D}|^2, \tag{5}$$

which is just as Eq. (4) but with the total Green function $\mathbf{G}$ replaced by its static part $\mathbf{G}_\mathrm{S}$ (defined below). From the above relations it follows that the question whether a change in the LDOS will affect the energy transfer rate becomes a question about the properties of the Green function, which we discuss in the following.

For the energy transfer rate Eq. (3) we only need to know the Green function in the frequency interval where the donor and acceptor spectra overlap appreciably. We will assume that absorption and material dispersion can be neglected in this overlap region, so that $\varepsilon(\mathbf{r}, \omega)$ in the overlap region can be approximated by a real-valued frequency-independent dielectric function $\varepsilon(\mathbf{r})$. The corresponding Green function $\mathbf{G}(\mathbf{r}, \mathbf{r}', \omega)$ is the solution of

$$-\nabla \times \nabla \times \mathbf{G}(\mathbf{r}, \mathbf{r}', \omega) + \varepsilon(\mathbf{r})(\omega/c)^2 \mathbf{G}(\mathbf{r}, \mathbf{r}', \omega) = \delta(\mathbf{r} - \mathbf{r}')\mathbf{I}. \tag{6}$$

This is the usual wave equation for light, with a localized source on the right-hand side. Unlike $\varepsilon(\mathbf{r})$, the Green function $\mathbf{G}(\mathbf{r}, \mathbf{r}', \omega)$ is frequency-dependent and complex-valued.

In order to find a relation between the energy transfer rate and the LDOS, we will express the Green function in terms of the complete set of optical eigenmodes $\mathbf{f}_\lambda$ that satisfy the equation

$$-\nabla \times \nabla \times \mathbf{f}_\lambda(\mathbf{r}) + \varepsilon(\mathbf{r})(\omega_\lambda/c)^2 \mathbf{f}_\lambda(\mathbf{r}) = 0, \tag{7}$$

with eigenfrequencies $\omega_\lambda \geq 0$. For later use, note that Eq. (6) implies that the *imaginary part* of the Green function satisfies the same source-free equation (7) as the subset of modes $\mathbf{f}_\lambda(\mathbf{r})$ for which $\omega_\lambda = \omega$. Therefore, $\mathrm{Im}[\mathbf{G}(\mathbf{r}, \mathbf{r}', \omega)]$ can be completely expanded in terms of only those degenerate eigenmodes.

The mode-function expansion of the Green function consists of three terms [7],

$$\mathbf{G}(\mathbf{r}, \mathbf{r}', \omega) \;=\; \underbrace{c^2 \sum_\lambda \frac{\mathbf{f}_\lambda(\mathbf{r})\mathbf{f}_\lambda^*(\mathbf{r}')}{(\omega + \mathrm{i}\eta)^2 - \omega_\lambda^2}}_{\mathbf{G}_\mathrm{R}} \quad \underbrace{- \left(\frac{c}{\omega}\right)^2 \sum_\lambda \mathbf{f}_\lambda(\mathbf{r})\mathbf{f}_\lambda^*(\mathbf{r}')}_{\mathbf{G}_\mathrm{S}} + \frac{1}{\varepsilon(\mathbf{r})(\omega/c)^2}\delta(\mathbf{r} - \mathbf{r}')\mathbf{I}. \tag{8}$$

Since by Eq. (4) the Green function controls the energy transfer rate, it is useful discern energy transfer processes corresponding to these three terms. The first term on the right-hand side of Eq. (8) will be denoted by $\mathbf{G}_\mathrm{R}$ and corresponds to resonant dipole-dipole interaction (RDDI), the radiative process by which the donor at position $\mathbf{r}$ emits a photon, which is then absorbed by the acceptor at position $\mathbf{r}'$. Between emission and absorption (in principle) a photon could be detected. The name 'resonant' describes that photons close to resonance with the D/A energy are the more probable energy transporters, in line with the denominator $(\omega + \mathrm{i}\eta)^2 - \omega_\lambda^2$ of this first term. The second term in (8) will be called $\mathbf{G}_\mathrm{S}$ and corresponds to the static dipole-dipole interaction (SDDI), which also causes energy transfer from donor to acceptor, but by virtual (not necessarily resonant) photons. The SDDI gives rise to the Förster energy transfer rate that in homogeneous media characteristically scales as $|\mathbf{r}_\mathrm{A} - \mathbf{r}_\mathrm{D}|^{-6}$ and dominates the energy transfer for strongly subwavelength donor-acceptor separations. The third term in Eq. (4) is proportional to the Dirac delta function $\delta(\mathbf{r} - \mathbf{r}')$, does not contribute to energy transfer, and can be neglected in the following.

We will now use the mode expansion of the Green function to derive a new and useful expression, relating the Förster transfer rate to an integral over $\mathrm{Im}[\mathbf{G}]$. We will use the fact that $\mathbf{G}_\mathrm{S}(\mathbf{r}, \mathbf{r}', \omega)$ is real-valued, the proof of which is given in Ref. [8]. The proof is based on the fact that mode functions of a nondispersive nonabsorbing dielectric

medium in principle can be chosen real-valued. Thus the imaginary part of the Green function is equal to $\mathrm{Im}[\mathbf{G}_\mathrm{R}]$ and the mode expansion of $\mathrm{Im}[\mathbf{G}]$ becomes

$$\mathrm{Im}[\mathbf{G}(\mathbf{r},\mathbf{r}',\omega)] = -\frac{\pi c^2}{2\omega}\sum_\lambda \mathbf{f}_\lambda(\mathbf{r})\mathbf{f}_\lambda^*(\mathbf{r}')\delta(\omega-\omega_\lambda), \tag{9}$$

where $\omega > 0$ is assumed. Notice that indeed only degenerate modes with frequencies $\omega_\lambda = \omega$ show up here, in agreement with the argument below Eq. (7), and that the mode expansion (9) is indeed a solution of Eq. (7).

Now if we multiply the right-hand side with ω and then integrate over ω, we obtain an expression proportional to $\mathbf{G}_\mathrm{S}$, and we thereby find the central identity of this Supporting Material,

$$\mathbf{G}_\mathrm{S}(\mathbf{r}_\mathrm{A},\mathbf{r}_\mathrm{D},\omega) = \frac{2}{\pi\omega^2}\int_0^\infty \mathrm{d}\omega_1\,\omega_1\,\mathrm{Im}[\mathbf{G}(\mathbf{r}_\mathrm{A},\mathbf{r}_\mathrm{D},\omega_1)]. \tag{10}$$

It is a general result for a photonic medium, derived using a complete set of modes and independent of the set of modes used. When inserting this into Eq. (5) we obtain the Förster transfer amplitude $w_\mathrm{S}(\omega)$ and hence also the transfer rate W of Eq. (3) in terms of the imaginary part of the Green function, analogous to the well-known expression (2) for the spontaneous-emission rate. There are however two differences, a major and a minor one. The major difference between Eq. (10) for Förster energy transfer and Eq. (2) for spontaneous emission in terms of $\mathrm{Im}[\mathbf{G}]$ is of course that Eq. (10) is an *integral* over all possible frequencies. The difference that below will turn out to be minor is that in Eq. (10) the Green function $\mathrm{Im}[\mathbf{G}(\mathbf{r}_\mathrm{A},\mathbf{r}_\mathrm{D},\omega_1)]$ appears, with *two* position arguments, one for the donor and one for the acceptor. The advantage of an expression in terms of $\mathrm{Im}[\mathbf{G}]$ is that $\mathrm{Im}[\mathbf{G}]$, in contrast to $\mathrm{Re}[\mathbf{G}]$, does not diverge for $\mathbf{r}_\mathrm{A} \to \mathbf{r}_\mathrm{D}$. The identity (10) is important since our goal is to find the relation between the optical LDOS and the Förster energy transfer rate. With Eq. (10), both quantities can now be expressed in terms of the imaginary part of the Green function, which brings us close to our goal.

Let us now test the relation (10) for a homogeneous medium with $\varepsilon(\mathbf{r}) = n^2$ and $\mathbf{r} \equiv \mathbf{r}_\mathrm{A} - \mathbf{r}_\mathrm{D}$, for which the Green function has the imaginary part [9]

$$\mathrm{Im}[\mathbf{G}^\mathrm{hom}(\mathbf{r},\omega)] = \frac{\mathbf{I}-3\hat{\mathbf{r}}\otimes\hat{\mathbf{r}}}{4\pi r}\left[\frac{\sin(n\omega r/c)-(n\omega r/c)\cos(n\omega r/c)}{(n\omega r/c)^2}\right] - \frac{\mathbf{I}-\hat{\mathbf{r}}\otimes\hat{\mathbf{r}}}{4\pi r}\sin(n\omega r/c). \tag{11}$$

By inserting this into Eq. (10), the frequency integral over the first part $\propto (\mathbf{I}-3\hat{\mathbf{r}}\otimes\hat{\mathbf{r}})$ gives

$$\mathbf{G}_\mathrm{S}^\mathrm{hom}(\mathbf{r},\omega) = \frac{1}{(n\omega r/c)^2}\frac{\mathbf{I}-3\hat{\mathbf{r}}\otimes\hat{\mathbf{r}}}{4\pi r}, \tag{12}$$

which is the near-field expression $\propto 1/(n^2r^3)$ that upon inserting into Eqs. (3) and (5) leads to the well-known Förster transfer rate $\propto 1/(n^4r^6)$. The frequency integral over the second part $\propto (\mathbf{I}-\hat{\mathbf{r}}\otimes\hat{\mathbf{r}})$ of Eq. (11) gives a delta-function contribution that can be neglected for energy transfer. Thus it is reassuring to find for homogeneous media the well-known Förster transfer rate using our general formula Eq. (10).

FÖRSTER TRANSFER AND FREQUENCY-INTEGRATED LDOS

We will now use Eq. (10) to derive an approximate expression relating the Förster transfer rate to the frequency-integrated LDOS. To that end, note that $\mathrm{Im}[\mathbf{G}]$ for homogeneous media in Eq. (11) varies appreciably only on the wavelength scale of light ($\lambda_0 = 500\,\mathrm{nm}$; $\omega_0 = 2\pi c/\lambda_0$), whereas Förster energy transfer occurs on a length scale of 5 nm, so typically a hundred times smaller. Since $\mathrm{Im}[\mathbf{G}]$ satisfies the homogeneous equation (7) and in analogy with the property of homogeneous media, we will now assume that also in inhomogeneous media $\mathrm{Im}[\mathbf{G}]$ varies appreciably only on the wavelength scale of light. Then for typical Förster transfer D-A distances, the zero-order Taylor approximation in $\mathbf{r} \equiv \mathbf{r}_\mathrm{A} - \mathbf{r}_\mathrm{D}$ that $\mathrm{Im}[\mathbf{G}(\mathbf{r}_\mathrm{A},\mathbf{r}_\mathrm{D},\omega_1)]$ can be approximated by $\mathrm{Im}[\mathbf{G}(\mathbf{r}_\mathrm{D},\mathbf{r}_\mathrm{D},\omega_1)]$ will be accurate for frequencies up to $\Omega = 10\omega_0$, corresponding to a free-space wavelength as small as 50 nm. The specific value of Ω does not matter so much, more that it can be chosen much higher than optical frequencies while still the inequality $n\Omega|\mathbf{r}_\mathrm{A}-\mathbf{r}_\mathrm{D}|/c \ll 1$ holds. Within this approximation, the Förster transfer rate can be related to the LDOS, analogous to Eq. (2) for spontaneous-emission rates. The crucial difference is that the Förster transfer rate is given by the sum of two frequency integrals, since

$$\mathbf{G}_\mathrm{S}(\mathbf{r}_\mathrm{A},\mathbf{r}_\mathrm{D},\omega) = \frac{2}{\pi\omega^2}\int_0^\Omega \mathrm{d}\omega_1\,\omega_1\,\mathrm{Im}[\mathbf{G}(\mathbf{r}_\mathrm{D},\mathbf{r}_\mathrm{D},\omega_1)] + \frac{2}{\pi\omega^2}\int_\Omega^\infty \mathrm{d}\omega_1\,\omega_1\,\mathrm{Im}[\mathbf{G}(\mathbf{r}_\mathrm{A},\mathbf{r}_\mathrm{D},\omega_1)]. \tag{13}$$

Here the first term can be recognized as an integral over the LDOS, integrated over a large frequency interval ranging from the far infrared to far beyond optical frequencies. The validity of the approximate expression (13) improves as the D-A distance r is reduced, since then the zero-order Taylor expansion of $\mathrm{Im}[\mathbf{G}]$ in $(\mathbf{r}_\mathrm{A}-\mathbf{r}_\mathrm{D})$ is better. We can also improve the approximation (13) by choosing Ω smaller, and it coincides with the exact relation (10) for vanishing Ω.

We will now test the accuracy of the approximate expression (13) by taking the homogeneous medium as an example. By inserting $\mathrm{Im}[\mathbf{G}^\mathrm{hom}]$ of Eq. (11) into the right-hand side of Eq. (13), we obtain

$$\mathbf{G}_\mathrm{S}^\mathrm{hom}(\mathbf{r},\omega)=\frac{1}{(n\omega r/c)^2}\frac{1}{4\pi r}\left\{(\mathbf{I}-3\hat{\mathbf{r}}\otimes\hat{\mathbf{r}})\left[1-\frac{2(n\Omega r/c)^2}{9\pi}\right]+(\mathbf{I}-\hat{\mathbf{r}}\otimes\hat{\mathbf{r}})\left[\frac{(n\Omega r/c)^5}{15\pi}\right]\right\}. \tag{14}$$

The first thing to notice is that this differs from the exact result (12) by only a small amount, since $n\Omega r/c\ll 1$. Indeed we approach the exact result in the limits of vanishing r and Ω, as anticipated in the general case. Thus we find that the Förster transfer rate can be accurately expressed as a frequency integral that in the optical regime runs over the imaginary part of $\mathrm{Im}[\mathbf{G}(\mathbf{r}_\mathrm{D},\mathbf{r}_\mathrm{D},\omega)]$, the same Green-function quantity that determines spontaneous-emission rates. However, the by far dominant contribution $\propto 1/(n^2r^3)$ originates from the second, high-frequency integral ranging from Ω to infinity, and thus has not much to do with the optical LDOS. Furthermore, this dominant term stems from the part of $\mathrm{Im}[\mathbf{G}^\mathrm{hom}(\mathbf{r}_\mathrm{D},\mathbf{r}_\mathrm{D},\omega)]$ that is proportional to $(\mathbf{I}-3\hat{\mathbf{r}}\otimes\hat{\mathbf{r}})$, whereas the spontaneous-emission rate only depends on the term proportional to $(\mathbf{I}-\hat{\mathbf{r}}\otimes\hat{\mathbf{r}})$.

This all adds to the conclusion for homogeneous media that Förster transfer rates are quite unaffected by spontaneous-emission rates in the entire optical regime, even though we were able to show that both can be expressed in terms of the imaginary part of the Green function. The general arguments given above suggest that this conclusion also holds for general inhomogeneous media, where the effect of the LDOS may be even weaker since engineered enhancements or reductions of the optical spontaneous emission rates in photonic structures often average against effects in other frequency intervals. Also, a large but narrow-band effect on the LDOS in the optical regime only has a very limited effect on Förster energy transfer.

SCALING WITH D-A DISTANCE OF FÖRSTER TRANSFER RATE

Above we used the example of a homogeneous medium to illustrate our general results for Förster transfer in photonic media. Here we show that the homogeneous-medium Förster transfer rate, scaling as $\propto 1/(n_\mathrm{hom}^4 r^6)$, is an important limiting case also for inhomogeneous media.

Let us assume that the donor and acceptor are separated by a few nanometers distance, experiencing the same dielectric material with a dielectric function that we call ε_hom, within an inhomogeneous photonic environment. In all of space, we define the optical potential $\mathbf{V}(\mathbf{r},\omega)=-[\varepsilon(\mathbf{r})-\varepsilon_\mathrm{hom}](\omega/c)^2\mathbf{I}$, so that the optical potential vanishes in the vicinity of the donor-acceptor pair. Then the Green function of the medium can be expressed in terms of the homogeneous-medium Green function and the optical potential as

$$\mathbf{G}(\mathbf{r}_\mathrm{A},\mathbf{r}_\mathrm{D},\omega)=\mathbf{G}^\mathrm{hom}(\mathbf{r}_\mathrm{A}-\mathbf{r}_\mathrm{D},\omega)+\int \mathrm{d}\mathbf{r}_1\,\mathbf{G}^\mathrm{hom}(\mathbf{r}_\mathrm{A}-\mathbf{r}_1,\omega)\cdot\mathbf{V}(\mathbf{r}_1,\omega)\cdot\mathbf{G}(\mathbf{r}_1,\mathbf{r}_\mathrm{D},\omega), \tag{15}$$

which is the Dyson-Schwinger equation for the Green function that controls the energy transfer. The equation can be formally solved in terms of the T-matrix of the medium as

$$\mathbf{G}(\mathbf{r}_\mathrm{A},\mathbf{r}_\mathrm{D},\omega)=\mathbf{G}^\mathrm{hom}(\mathbf{r}_\mathrm{A}-\mathbf{r}_\mathrm{D},\omega)+\int\int \mathrm{d}\mathbf{r}_1\mathrm{d}\mathbf{r}_2\,\mathbf{G}^\mathrm{hom}(\mathbf{r}_\mathrm{A}-\mathbf{r}_1,\omega)\cdot\mathbf{T}(\mathbf{r}_1,\mathbf{r}_2,\omega)\cdot\mathbf{G}^\mathrm{hom}(\mathbf{r}_2-\mathbf{r}_\mathbf{D},\omega). \tag{16}$$

The important property of the T-matrix $\mathbf{T}(\mathbf{r}_1,\mathbf{r}_2,\omega)$ is now that it is only non-vanishing where both $\mathbf{V}(\mathbf{r}_1)$ and $\mathbf{V}(\mathbf{r}_2)$ are nonzero, so that it vanishes in the vicinity of the donor-acceptor pair. Thus the Green function that controls the energy transfer is given by a homogeneous-medium Green function and a scattering term. The former is a function of the distance between donor and acceptor, whereas the latter does not depend on the D-A distance, but rather on the distance of donor and acceptor to points in space where the optical potential is non-vanishing.

As the D-A distance is decreased, the homogeneous-medium contribution in Eq. (16) grows rapidly, essentially becoming equal to $\mathbf{G}_\mathrm{S}^\mathrm{hom}(\mathbf{r}_\mathrm{A}-\mathbf{r}_\mathrm{D},\omega)$ of Eq. (12), whereas the contribution of the scattering term does not change much. So in the limit of very small D-A separations, the homogeneous-medium term always wins, and one would find the well-known Förster transfer rate of the infinite homogeneous medium $\propto 1/(n_\mathrm{hom}^4 r^6)$. For general photonic media one cannot say at what separation the homogeneous-medium term starts to dominate. Smaller D-A distances are needed before this dominance sets in if donor and acceptor are located closer to an interface with a medium with larger refractive-index difference compared to n_hom. The important point is that the homogeneous-medium Förster transfer rate is the small-distance limit also for Förster transfer in inhomogeneous media.

CONCLUSIONS OF PART II: BACKGROUND THEORY

We have studied the connection between Förster energy transfer and spontaneous-emission rates in a nondispersive photonic medium, by expressing both rates in terms of the imaginary part of the Green function of the medium. We find that Förster energy transfer can be expressed as a frequency integral over the imaginary part of the Green function, and that in the optical regime and beyond, the Green function $\mathrm{Im}[\mathbf{G}(\mathbf{r}_\mathrm{A},\mathbf{r}_\mathrm{D},\omega)]$ in the integrand can be replaced by $\mathrm{Im}[\mathbf{G}(\mathbf{r}_\mathrm{D},\mathbf{r}_\mathrm{D},\omega)]$, which is proportional to the optical LDOS, the same quantity that controls spontaneous-emission rates. However, for homogeneous media we have seen that the by far dominant contribution to Förster energy transfer is not this integral over the LDOS, but rather the high-frequency integral over $\mathrm{Im}[\mathbf{G}(\mathbf{r}_\mathrm{A},\mathbf{r}_\mathrm{D},\omega)]$. We argued that the same holds true for general inhomogeneous media. We also found that the homogeneous-medium Förster transfer rate $\propto 1/(n_\mathrm{hom}^4 r^6)$ is the small-distance limit also for Förster transfer in inhomogeneous media, where n_hom is the refractive index surrounding the donor-acceptor pair. Our theoretical findings support the experimental results of the main text, namely that Förster energy transfer rates are practically unaffected by changing the optical LDOS, when keeping fixed the subwavelength local dielectric environment of the donor-acceptor pair.

* Email: c.blum@utwente.nl

[1] M. Maus, M. Cotlet, J. Hofkens, T. Gensch, F. C. De Schryver, J. Schaffer, and C. A. M. Seidel, *An Experimental Comparison of the Maximum Likelihood Estimation and Nonlinear Least-Squares. Fluorescence Lifetime Analysis of Single Molecules*, Anal. Chem. **73**, 2078 (2001).

[2] Y. Cesa, C. Blum, J. M. van den Broek, A. P. Mosk, W. L. Vos, and V. Subramaniam, *Manipulation of the local density of photonic states to elucidate fluorescent protein emission rates*, Phys. Chem. Chem. Phys. **11**, 2525 (2009).

[3] D. G. Norman, R. J. Grainger, D. FUhrin, and D.M.J. Lilley, *Location of Cyanine-3 on Double-Stranded DNA: Importance for Fluorescence Resonance Energy Transfer Studies*, Biochem. **39**, 6317 (2000).

[4] J.J. Rindermann, Y. Akhtman, J. Richardson, T. Brown, and P. G. Lagoudakis, *Gauging the Flexibility of Fluorescent Markers for the Interpretation of Fluorescence Resonance Energy Transfer*, J. Am. Chem. Soc. **133**, 279 (2011).

[5] H. T. Dung, L. Knöll, and D.-G. Welsch, *Intermolecular energy transfer in the presence of dispersing and absorbing media*, Phys. Rev. A **65**, 043813 (2002).

[6] V. May and O. Kühn, *Charge and energy transfer dynamics in molecular systems* (Wiley, Berlin, 2000).

[7] M. Wubs, L. G. Suttorp, and A. Lagendijk, *Multiple-scattering approach to interatomic interactions and superradiance in inhomogeneous dielectrics*, Phys. Rev. A **70**, 053823 (2004).

[8] M. Wubs, L. G. Suttorp, and A. Lagendijk, *Multipole interaction between atoms and their photonic environment*, Phys. Rev. A **68**, 013822 (2003).

[9] P. de Vries, D. V. van Coevorden, and A. Lagendijk, *Point scatterers for classical waves*, Rev. Mod. Phys. **70**, 447 (1998).